American Society of Hematology
2021 L Street NW, Suite 900,
Washington, DC 20036
Phone: 202-776-0544 | Fax 202-776-0545
editorial@hematology.org

Tracing the evolutionary history of blood cells to the unicellular ancestor of animals

Tracking no: BLD-2022-016286R2

Yosuke Nagahata (Kyoto University, Japan) Kyoko Masuda (Kyoto University, Japan) Yuji Nishimura (Kyoto University, Japan) Tomokatsu Ikawa (Tokyo University of Science, Japan) Shinpei Kawaoka (Kyoto University, Japan) Toshio Kitawaki (Graduate School of Medicine, Kyoto University, Japan) Yasuhito Nanya (University of Tokyo, Japan) Seishi Ogawa (Kyoto University, Japan) Hiroshi Suga (Prefectural University of Hiroshima, Japan) Yutaka Satou (Graduate School of Science, Kyoto University, Japan) Akifumi Takaori-Kondo (Graduate School of Medicine, Kyoto University, Japan) Hiroshi Kawamoto (Kyoto University, Japan)

Abstract:
Blood cells are thought to have emerged as phagocytes in the common ancestor of animals followed by the appearance of novel blood cell lineages such as thrombocytes, erythrocytes, and lymphocytes, during evolution. However, this speculation is not based on genetic evidences and it is still possible to argue that phagocytes in different species have different origins. It also remains to be clarified how the initial blood cells evolved: whether ancient animals have solely developed *de novo* programs for phagocytes, or they have inherited a key program from ancestral unicellular organisms. Here we traced the evolutionary history of blood cells, and cross-species comparison of gene expression profiles revealed that phagocytes in various animal species and Capsaspora, a unicellular organism, are transcriptionally similar to each other. We also found that both phagocytes and Capsaspora share a common phagocytic program, and that CEBPa is the sole transcription factor highly expressed in both phagocytes and Capsaspora. We further showed that the function of CEBPa to drive phagocyte program in non-phagocytic blood cells has been conserved in tunicate, sponge and Capsaspora. We finally showed that, in murine hematopoiesis, repression of CEBPa to maintain non-phagocytic lineages is commonly achieved by polycomb complex. These findings indicate that the initial blood cells emerged inheriting a unicellular organism program driven by CEBPa and that the program has been also seamlessly inherited in phagocytes of various animal species throughout evolution.

Conflict of interest: No COI declared

COI notes:

Preprint server: No;

Author contributions and disclosures: Y.Nagahata and H.K. designed the project. Y.Nagahata, H.S., and Y.S. performed experiments. Y.Nagahata, K.M., Y.Nishimura, T.I., S.K., T.K., Y.Nannya, S.O., and A.T.-K. contributed vital new reagents or analytical tools. Y.Nagahata, H.S., Y.S. analyzed the data. Y.Nagahata., K.M., and H.K. wrote the paper.

Non-author contributions and disclosures: Yes; Peter Burrows (University of Alabama at Birmingham) contributed with critical reading and proofreading of the manuscript, and his assistance was supported by funds from Japan Society for the Promotion of Science KAKENHI, Grant-in-Aid for Scientific Research on Innovative Areas (JP 19H05747).

Agreement to Share Publication-Related Data and Data Sharing Statement: Correspondence and requests for materials and data should be addressed to Hiroshi Kawamoto (kawamoto@infront.kyoto-u.ac.jp). Primary RNA sequencing data of tunicate phagocytes and Ring1a/b KO myeloid cells were available at DNA Data Bank of Japan (DDBJ) database (DRA013007, and DRA014437).

Clinical trial registration information (if any):

Tracing the evolutionary history of blood cells to the unicellular ancestor of animals

Short title: The evolutionary origin of blood cells

Science category: Phagocytes, Granulocytes, and Myelopoiesis

Yosuke Nagahata[1,2], Kyoko Masuda[1], Yuji Nishimura[1], Tomokatsu Ikawa[3], Shinpei Kawaoka[4], Toshio Kitawaki[2], Yasuhito Nannya[5], Seishi Ogawa[5], Hiroshi Suga[6], Yutaka Satou[7], Akifumi Takaori-Kondo[2], Hiroshi Kawamoto[1]*

1. Laboratory of Immunology, Institute for Life and Medical Sciences, Kyoto University, Kyoto, 606-8507, Japan
2. Department of Hematology and Oncology, Graduate School of Medicine, Kyoto University, Kyoto, 606-8397, Japan
3. Division of Immunology and Allergy, Research Institute for Biomedical Sciences, Tokyo University of Science, Chiba, 278-0022, Japan
4. Inter-Organ Communication Research Team, Institute for Life and Medical Sciences, Kyoto University, Kyoto, 606-8507, Japan
5. Department of Pathology and Tumor Biology, Graduate School of Medicine, Kyoto University, Kyoto, 606-8501, Japan
6. Department of Life and Environmental Sciences, Prefectural University of Hiroshima, Shobara, 727-0023, Japan
7. Department of Zoology, Graduate School of Science, Kyoto University, Kyoto,

606-8502, Japan

*Corresponding Author: Hiroshi Kawamoto

53 Kawahara-cho, Shogoin, Sakyo-ku, Kyoto 606-8507, Japan,

Phone: (81)-75-751-3815

Fax: (81)-75-751-3839

Email: kawamoto@infront.kyoto-u.ac.jp

Text: 4357 words

Abstract: 230 words

7 Figures, 17 supplemental Figures, and 9 supplemental Tables

92 references including 19 supplemental references (# 74-92)

Key Points

The initial blood cells emerged in the common ancestor of animals inheriting a phagocytic program from unicellular organisms.

In murine hematopoiesis, CEBPα is commonly repressed by polycomb complexes to maintain non-phagocytic lineages.

Abstract

Blood cells are thought to have emerged as phagocytes in the common ancestor of animals followed by the appearance of novel blood cell lineages such as thrombocytes, erythrocytes, and lymphocytes, during evolution. However, this speculation is not based on genetic evidences and it is still possible to argue that phagocytes in different species have different origins. It also remains to be clarified how the initial blood cells evolved: whether ancient animals have solely developed *de novo* programs for phagocytes, or they have inherited a key program from ancestral unicellular organisms. Here we traced the evolutionary history of blood cells, and cross-species comparison of gene expression profiles revealed that phagocytes in various animal species and Capsaspora, a unicellular organism, are transcriptionally similar to each other. We also found that both phagocytes and Capsaspora share a common phagocytic program, and that CEBPα is the sole transcription factor highly expressed in both phagocytes and Capsaspora. We further showed that the function of CEBPα to drive phagocyte program in non-phagocytic blood cells has been conserved in tunicate, sponge and Capsaspora. We finally showed that, in murine hematopoiesis, repression of CEBPα to maintain non-phagocytic lineages is commonly achieved by polycomb complex. These findings indicate that the initial blood cells emerged inheriting a unicellular organism program driven by CEBPα and that the program has been also seamlessly inherited in phagocytes of various animal species throughout evolution.

Introduction

Among various lineage blood cells, such as erythrocytes and lymphocytes, phagocytes including macrophages and neutrophils have been thought to represent the most evolutionarily ancient blood cells, since phagocytes can be found in any animals including morphologically very simple multicellular organisms like the sponge[1], while more lineage types can be seen in more complex animals[2-5]. It has been thus speculated that the evolutionary initial blood cells emerged as phagocytes in the common ancestor of animals, and that various non-phagocyte lineages have evolved from the primordial phagocytes during evolution. Concerning this issue, we have demonstrated that the potential to produce phagocytes is retained in the early progenitors primed for erythroid, T and B cell lineages in murine hematopoiesis[6-10]. Based on such findings, we have proposed that the retention of phagocyte potential in these lineage progenitors is a vestige of the phylogenic process, where each of these lineages has evolved from ancestral phagocytes[2,11]. The vestige has also been found in other vertebrates: thrombocytes, erythrocytes, and B cells in shark, bony fish, and frog have phagocytic potential[12-14].

One thing to note here is that such speculation can be done provided that all phagocytes have the same origin during phylogeny. However, genetic evidence supporting this model has been insufficient, and we can still argue a possibility of convergent evolution: phagocytes in different animal species have different origins. Furthermore, it also remains to be clarified how the initial blood cells evolved. We can argue two possible cases; the first is that ancient animals have solely developed *de novo* programs for phagocytes, and the second is that they inherited a key program from ancestral unicellular organisms.

To address this issue, we decided to clarify whether or not a common program has been shared in phagocytes of various animal species and whether the program is also shared with a unicellular organism. To this end, we compared gene expression profiles in phagocytes and non-phagocytes of various animal species, and unicellular organisms.

Methods

Mice

Ert2Cre-Cdkn2a$^{-/-}$*Ring1a*$^{-/-}$*Ring1b*$^{fl/fl}$, *Ert2Cre-CAG*$^{flox\text{-}stop\text{-}GFP}$*-Cdkn2a*$^{-/-}$*Ring1a*$^{-/-}$*Ring1b*$^{fl/fl}$, and *LckCre-Cdkn2a*$^{-/-}$*Ring1a*$^{-/-}$*Ring1b*$^{fl/fl}$ mice were generated and maintained in our animal facility. All mice were maintained in SPF conditions in our animal facility. All experiments were performed in accordance with the guidelines of the Kyoto University Animal Experiment Committee and approved by our institutional committee.

Tunicate

Ciona intestinalis (type A; also called *Ciona robusta*) adults were obtained from the National BioResource Project for *Ciona*.

Capsaspora

Capsaspora owczarzaki were maintained at 23°C in the ATCC 1034 medium as previously reported [15].

Data and code availability

Public data of mouse in EMBL-EBI (supplemental Table 1) and data of mouse, tunicate, sponge, Capsaspora, *Salpingoeca rosetta*, and *Creolimax fragrantissima* in previous reports were analyzed[15-23]. RNA sequencing data of tunicate phagocytes and *Ring1a/b*

KO myeloid cells were available at DNA Data Bank of Japan (DDBJ) database (DRA013007, and DRA014437).

Cross-species transcriptomic comparison

We identified homologs in *M. musculus*, *C. intestinalis*, *A. queenslandica*, and *C. owczarzaki* using the OrthoFinder (supplemental Table 2)[24]. Homolog groups commonly conserved across the four species were selected and used for cross-species comparison (supplemental Table 3). Cross species analysis of six species adding *S. rosetta* and *C. fragrantissima* was also performed (supplemental Table 4-5).

TFs and phagocytosis related genes

For selecting TFs and phagocytosis/lysosome related genes, we used the AmiGO2 database (http://amigo.geneontology.org/amigo) (supplemental Table 6).

Isolation of mouse progenitors

Single-cell suspensions of the thymus or bone marrow (BM) were prepared and progenitors were isolated by FACS. Gating strategies are shown in supplemental Figure 1.

CEBPα encoding vectors

Codon optimized CEBPα and Ring1B were synthesized using GeneArt (Thermo Fisher Scientific) (supplemental Table 7).

Retrovirus production and transduction

CEBPα and Ring1B encoding vectors were transfected into the Plat-E cells (CosmoBio) and supernatants were harvested. For transduction, purified progenitors were resuspended with the supernatant, and were centrifuged for 90 min at 1,000 g at 32℃.

Phagocytosis assay

pHrodo-green zymosan or *S. aureus* beads (Invitrogen) were added to each culture. One hour later, medium was replaced with PBS and phagocytosis was observed using a fluorescence microscope.

RNA extraction and RT–qPCR

Total RNA was isolated using an RNeasy kit (Qiagen). cDNA synthesis was performed using a SuperScript IV VILO Master Mix cDNA synthesis kit (Invitrogen). Realtime PCR was performed using PowerUp SYBR Green Master Mix (Applied Biosystems) and analyzed by StepOnePlus (Applied Biosystems).

RNA sequencing of tunicate phagocytes and *Ring1a/b* KO myeloid cells

Libraries were prepared using SMART-Seq v4 Ultra Low Input RNA Kit for Sequencing (Takara) and Nextera XT DNA library Prep Kit (Illumina) and sequenced on a NovaSeq 6000 (Illumina).

In vitro* deletion of *Ring1b

The isolated progenitors were co-cultured with TSt4[25] or TSt4-DLL1[26] cells for 4-12 days, and *Ring1b* was deleted by 4-OHT.

Bone marrow chimera mice

Hemolyzed whole bone marrow cells (2×10^6 cells) were intravenously injected into sublethally irradiated (4 Gy) *Rag2*$^{-/-}$ mice. For long term observation, 1×10^6 bone marrow cells were transplanted with 1×10^6 competitor cells.

Statistical analysis

Survival rates were estimated using Kaplan-Meier methods and compared using Log-rank tests. Continuous and categorical variables were compared using 2-tailed t tests and Fisher's exact test, respectively.

Data Sharing Statement

Expression levels of homologs were found in supplemental Table 3 and 5. Other sources were also available with the online version of this article.

Further experimental details are provided in supplemental methods.

Results

Phagocytes of mouse, tunicate, and sponge are transcriptionally similar with a unicellular organism

We compared gene expression profiles of various lineage or stage cells among four species: mouse (*Mus musculus*), tunicate (*Ciona intestinalis*), sponge (*Amphimedon queenslandica*), and *Capsaspora owczarzaki*, a unicellular organism (hereafter Capsaspora) (Figure 1A). Among invertebrates, we selected tunicate and sponge because tunicate belongs to chordates and is close to vertebrates, whereas sponge is the animal oldest and farthest from vertebrates[27,28]. Among unicellular organisms, Capsaspora was selected because it is phylogenetically close to animals forming a clade termed Holozoa together with Metazoa (Figure 1A)[29-31]. We first searched homologs conserved among the four species and 3237 homolog groups were identified: 5911 genes in mouse, 4031 genes in tunicate, 5443 genes in sponge, and 4096 genes in Capsaspora were assigned to the 3237 homolog groups. Then gene expression profiles were compared based on the homolog groups (supplemental Figure 2A). As expected, mouse, tunicate, sponge and Capsaspora were very different form each other (supplemental Figure 2B). Among blood cells, macrophages were more similar with Capsaspora than non-phagocytic cells were (Figure 1C-D). Macrophages were also more similar with Capsaspora than neutrophils, in line with the fact that neutrophils

185 with multi-lobulated nuclei are unique to vertebrates[32]. In order to exclude batch effect
186 between mouse data sets, comparison using a single dataset of mouse cells with CAGE
187 method was also performed (Figure 1C). In the both analysis with RNA-seq and CAGE
188 datasets, macrophages, hepatocytes, fibroblast, and adipocyte showed high similarity to
189 Capsasapora among mouse cells (Figure 1B-C). Since, hepatocytes, fibroblast and
190 adipocyte are known to have phagocytic potential[33-35], macrophages and these 3 lineage
191 cells can be categorized as phagocytes. In principle component (PC) analysis,
192 phagocytes of mouse and tunicate, sponge archaeocytes which are known to have
193 phagocytic potential[1], and Capsaspora showed similarity to each other (Figure 1D).

194 Next, we examined how frequently Capsaspora and mouse various cell lineages
195 share highly expressed genes; number of genes expressed higher than embryonic stem
196 cells (ESCs) were examined. Capsaspora and macrophages highly expressed 325 and
197 545 genes, respectively, and they shared 101 genes (Figure 1E). Macrophages shared
198 more genes with Capsaspora than other blood cell lineages (Figure 1F; supplemental
199 Figure 3-4). Hepatocytes also shared many genes with Capsaspora, and also shared
200 more with macrophages among non-blood cells (supplemental Figure 3-4). KEGG
201 pathway analysis showed that lysosome-related genes were involved in genes shared by
202 Capsaspora, macrophages, and hepatocytes (supplemental Figure 5). Gene ontology
203 analysis using AmiGO2 database showed that 325 genes highly expressed in
204 Capsaspora more frequently contained phagocytosis/lysosome-related genes than 2252
205 low expressed genes (Figure 1G). These data suggested that phagocytosis- and
206 lysosome- related genes shape the similarity between Capsaspora and mouse
207 phagocytes. In fact, Capsaspora cells showed mouse macrophage-like cytology with
208 several vacuoles in cytoplasm (Figure 1H) and robust phagocytic activity (Figure 1I-J).

These data suggested that transcriptional profile of phagocytes has been conserved from common ancestors of Capsaspora and animals.

Phagocytes and a unicellular organism share a CEBPα-driven phagocytic program

Next, we compared gene expression profiles of Capsaspora and mouse macrophages with mouse ESCs and non-phagocytic blood cells: LSK cells, T cells, B cells, megakaryocytes, and erythroid cells. Eleven genes were highly expressed in both mouse macrophages and Capsaspora (Figure 2A; supplemental Figure 6A), and lysosome-related genes were involved in the 11 genes suggesting that these genes contribute to phagocytosis in phagosome/lysosome pathway (Figure 2B; supplemental Figure 6B). Nine of the 11 genes were also highly expressed in hepatocytes (supplemental Figure 6A). Next, we attempted to reveal which transcription factors (TFs) commonly play a key role in both Capsaspora and mouse phagocytes. We found 62 TFs were conserved among the four species, and then compared their expression levels. As with the case of the comparison based on the 3237 conserved genes (Figure 1B-C), comparison based on the 62 conserved TFs showed that mouse phagocytes were closer to Capsaspora than mouse non-phagocytes were (Figure 2C; supplemental Figure 7A-B). CEBPα was the sole TF highly expressed in both Capsaspora and mouse macrophages compared with mouse ESCs and non-phagocytic blood cells (Figure 2D-F; supplemental Figure 8A). Several regions of the CEBPα homologs, especially DNA binding bZIP domain, were conserved among the four species (supplemental Figure 9). Some other TFs were conserved among the four species (supplemental Figure 8B), and CEBPγ, the other CEBP homolog, was also examined because we were not

able to distinguish which was a functional CEBPα homolog in phylogenetic tree (supplemental Figure 10). However, we found that expression levels of CEBPγ were not highly expressed in Capsaspora (supplemental Figure 8C). Expression levels of GATA1-6 homologs in Capsaspora, macrophages, and hepatocytes were lower than megakaryocytes and erythroid cells (supplemental Figure 8D), and those of EBF1-4 were lower than B cells (supplemental Figure 8E). Relatively high expression levels of GATA and EBF families in Capsaspora and some mouse non-hematopoietic cells suggested that these TFs determine programs conserved among Capsaspora and mouse non-hematopoietic lineages[36-38]. Although PU.1 and IRF are important in murine myeloid cells[39,40], their homologs were not detected in Capsaspora (supplemental Figure 8B). When gene expression levels were compared between the three stages of Capsaspora, CEBPα was expressed higher in filopodial or cystic stages than aggregative stage (Figure 2F). Among the 11 genes highly expressed in mouse macrophages and Capsaspora, PLA2G15 was also expressed higher in filopodial and cystic stages (Figure 2F; supplemental Figure 6A). PLA2G15 is a lysosomal protein and plays roles in host defense and efferocytosis by human phagocytes[41,42]. These data suggested that a CEBPα-driven phagocytic program including PLA2G15 expression has been conserved from a unicellular organism to vertebrates.

We also performed cross-species analysis adding a Choanoflagellate (*Salpingoeca rosetta*) and Ichthyosporea (*Creolimax fragrantissima*). In this analysis, phagocytes of various species also showed similarity to each other and to unicellular organisms (supplemental Figure 11A-C). In mouse cell lineages, macrophages and adipocytes showed high similarity to unicellular organisms (supplemental Figure B-C).

Hgd was highly expressed in mouse macrophages, Capsaspora, and *C. fragrantissima* (supplemental Figure 11D). However, because both *S. rosetta* and *C. fragrantissima* lack CEBPα, no TFs highly expressed in all of mouse macrophages, Capsaspora, and *C. fragrantissima* were detected. Some important genes other than CEBPα may determine the similarity of these cells.

Tunicate and sponge phagocytes highly express CEBPα homologs

Next, we examined whether expression levels of CEBPα were different between phagocytes and non-phagocytic blood cells in sponge and tunicate. In sponges, we focused on archaeocytes, which behave like blood cells: they circulate around the body cavity and have phagocytic potential[1]. Analysis of archaeocytes showed that CEBPα expression levels were positively correlated with those of phagocytosis-related genes and PLA2G15, but CEBPγ levels were not (Figure 3A).

We also examined tunicate blood cells and their expression of CEBP homologs and phagocytosis related genes. CEBPα and phagocytosis related genes were highly expressed in the blood cells, especially in phagocytes, but CEBPγ was not (Figure 3B). In order to investigate whether CEBPα is differently expressed among various blood lineage cells in tunicate, we collected blood cells from tunicates (Figure 3C). The blood cells were then sorted into four fractions based on characteristics of i) small size (hemoblasts), ii) autofluorescence (morula cells), iii) fluorescence of engulfed beads (phagocytes), and iv) negative for these features (other blood cells) (Figure 3D). We found that the expression levels of CEBPα and PLA2G15 were remarkably higher in phagocytes compared to other lineages of blood cells, while that of CEBPγ was not or

slightly (Figure 3E). These data may indicate that, in both sponge and tunicate, CEBPα commonly exert phagocyte program.

Function of CEBPα to drive the phagocyte program has been conserved from a unicellular organism

We then asked if CEBPα of the tunicate, sponge and Capsaspora has a function similar to mouse CEBPα, whose enforced expression has been shown to convert T and B cells into phagocytes[43-46]. First, mouse proB cells were transduced with CEBPα of mouse, tunicates, sponge, and Capsaspora (Figure 4A). CEBPα of tunicate and sponge converted these B progenitors into cells that express CD11b as well as mouse CEBPα did, whereas the CEBPα of Capsaspora, and CEBPγ of sponge and Capsaspora, did not (Figure 4B; supplemental Figure 12A). The majority of the $CD11b^+$ cells induced by either of tunicate or sponge CEBPα looked like macrophages and showed efficient phagocytic activity (Figure 4C-D). D-J rearranged *Igh* genes were present in the generated $CD11b^+$ cells (supplemental Figure 12B), indicating that they were derived from proB cells. In order to clarify whether CEBPα of Capsaspora has the potential to drive the phagocyte program, we further examined other lineage progenitors. Megakaryocyte progenitors (MkPs), erythroid progenitors (ErPs), and double negative (DN) 3 T cell progenitors were examined, and CEBPα of Capsaspora as well as that of mouse, tunicate, and sponge converted MkPs into $CD11b^+$ phagocytes while CEBPγ of Capsaspora did not (Figure 4E-G; supplemental Figure 12C), indicating that Capsaspora CEBPα has the potential to drive the phagocytic program. We also found that CEBPα of mouse, tunicate, sponge, and Capsaspora converted ErPs into $CD11b^+$ cells (Figure

4H; supplemental Figure 12D). DN3 T progenitors were converted into $CD11b^+$ cells by mouse and sponge CEBPα, but not by the tunicate and Capsaspora homologs (Figure 4I; supplemental Figure 12E).

We then examined how functionally similar the CEBPα homologs were. CEBPα is known to play roles in the differentiation of mouse neutrophils, and indeed, mouse CEBPα converted proB cells into neutrophil-like cells with ring-shaped or multi-lobulated nuclei, while CEBPα of tunicate and sponge hardly did so (Figure 4J-K). The expression levels of various genes were also compared between proB cells transduced with the mouse and sponge CEBPα, which converted proB cells into phagocytes to a similar extent (Figure 4B). To examine the direct consequence of *Cebpa* gene expression, we collected the cells on day 2, when they had not yet begun to express CD11b (supplemental Figure 12F-G). Sponge CEBPα upregulated phagocyte-associated genes to the same extent as mouse CEBPα, but mouse CEBPα was superior to sponge CEBPα in inducing expression of neutrophil-associated genes and in repressing B cell-associated genes (Figure 4L; supplemental Figure 12H).

Polycomb mediated suppression of CEBPα is required for maintenance of various hematopoietic lineages in mouse

In mouse blood cells, CEBPα functions as master regulators of phagocytes, or myeloid cells in other words, having the potential to convert non-phagocytic lineage progenitors into myeloid cells[43-50], implying that CEBPα must be strictly repressed for maintenance of non-phagocytic lineages. We attempted to reveal how CEBPα is repressed in non-phagocytic lineage cells, and hypothesized that the polycomb complex, one of

major epigenetic repressors[51], plays a role in suppression of the phagocyte program. We focused on Ring1A and B, which are catalytic components of polycomb complex[52]. Expression levels of Ring1B were higher in non-phagocytic lineages than in myeloid cells reciprocally to those of CEBPα (supplemental Figure 13A-B). By analyzing published data, the *Cebpa* locus encoding CEBPα was found to be heavily marked with H3K27me3 in DN3 cells, proB cells, ErPs, and MkPs, but not in myeloid cells (supplemental Figure 13C). On the other hand, *Spi1* locus encoding PU.1 was found not to be marked with H3K27me3 (supplemental Figure 13D). We also observed Ring1B binding at the *Cebpa* locus (supplemental Figure 13E). In order to confirm that CEBPα is suppressed by polycomb, we deleted *Ring1b* by using 4-OHT in progenitors of each lineage from *Ert2Cre -Cdkn2a*$^{-/-}$*Ring1a*$^{-/-}$*Ring1b*$^{fl/fl}$ mice (supplemental Figure 13F). In this experiment, we used *Cdkn2a*$^{-/-}$ background mice because *Ring1a/b* knock out (KO) may cause derepression of Cdkn2a, leading to apoptosis of *Ring1a/b* deleted cells[53]. Upon deletion of *Ring1b*, expression levels of CEBPα were remarkably elevated within a few days in all lineages (supplemental Figure 13G). These data indicate that polycomb complex commonly suppresses CEBPα in various non-phagocytic lineages.

Next, we examined whether polycomb-mediated CEBPα suppression is physiologically important or not. We made BM chimera mice by transplantation of BM cells from *Ert2Cre-CAG*$^{flox\text{-}stop\text{-}GFP}$*-Cdkn2a*$^{-/-}$*Ring1a*$^{-/-}$*Ring1b*$^{fl/fl}$ mice into sublethally irradiated *Rag2*$^{-/-}$ mice. Six weeks after transplantation, *Ring1b* was deleted by administration of tamoxifen, and mice were analyzed 2 weeks later (Figure 5A). The number of thymocytes, double positive (DP) cells, DN cells, and DN3 cells in the GFP^{+} fraction was decreased, while that of DN1 cells was increased in the *Ring1a/b* KO BM

chimera mice (Figure 5B, E; supplemental Figure 14A-B, E). We also found a decrease in the number of proB cells and an increase of the number of B-1 progenitors, defined as $CD19^{+}B220^{-}$ cells (Figure 5C, F; supplemental Figure 14F). $Lin^{-}Sca1^{+}ckit^{+}$ (LSK) cells including hematopoietic stem cells were decreased, while $Lin^{-}Sca1^{-}ckit^{+}$ (LK) cells were increased (supplemental Figure 14C, G). The proportion of ErPs and MkPs was decreased, while common myeloid progenitors (CMPs) were increased, and Megakaryocyte-erythroid progenitors (MEPs) were intact (Figure 5D, G; supplemental Figure 14D, H).-Because hematopoiesis of the BM chimera mice was severely impaired, they died within a few months (Figure 5H).

To evaluate the long-term effect of *Ring1a/b* KO in blood cells, we performed transplantation of *Ring1a/b* KO BM cells with competitor BM cells, which should contribute normal hematopoiesis (Figure 5I). Eight weeks after deletion of *Ring1b*, almost all GFP^{+} *Ring1a/b* KO cells became $CD11b^{+}$ myeloid cells (Figure 5J-K). Furthermore, the BM of *Ring1a/b* KO mice was occupied with myeloid cells and exhibited an anemic appearance, and they died within three months (Figure 5L; supplemental Figure 15A-D). These GFP^{+} *Ring1a/b* KO myeloid cells expressed CD34, and looked like immature blasts (supplemental Figure 15E-F). Various lineage progenitors of thymocytes and BM cells, including competitor cells, were decreased, indicating that *Ring1a/b* KO myeloid cells were transformed into leukemic blasts and disturbed normal hematopoiesis (supplemental Figure 15G-L). We then examined whether sole *Ring1a/b* KO without *Cdkn2a* KO causes leukemia or not. We found that mice with $Cdkn2a^{+/-}Ring1a^{-/-}Ring1b^{\Delta/\Delta}$ cells did not develop leukemia, and GFP^{+} cells disappeared (Figure 5J; supplemental Figure 15D). This result suggested that the KO of *Ring1a/b*, leaving $Cdkn2a^{+/-}$ still present, led to overexpression of Cdkn2a, resulting in

apoptosis of KO cells as previously reported in the T-cell specific KO case[53].

Various lineage progenitors were reverted into the primordial lineage of phagocytes by *Ring1a/b KO*

In BM chimera mice, we showed that the number of various lineage progenitors was decreased while that of myeloid cells was increased (Figure 5). Next, we tested whether cell fate conversion from each of the lineage progenitors into myeloid cells had occurred or not. First, we found that the myeloid cells from the *Ring1a/b* KO mice carried rearranged IgH genes, but those of control mice showed no rearrangements (supplemental Figure 16A). Among eight *Ring1a/b* KO BM chimera mice examined, five carried IgH-rearranged myeloid cells. These data indicate that B cells were converted into myeloid cells *in vivo*. In order to examine whether various lineage progenitors are converted into myeloid cells by *Ring1a/b* KO, DN3 cells, proB cells, ErPs, and MkPs of *Ert2Cre-Cdkn2a*$^{-/-}$*Ring1a*$^{-/-}$*Ring1b*$^{fl/fl}$ mice were cultured with or without 4-OHT (Figure 6A). Since these progenitors had already been determined to their respective lineages, control cells maintained their lineage identity (Figure 6B). On the other hand, by deletion of *Ring1b*, these progenitors gave rise to CD11b^{+} macrophage-like cells (Figure 6B-C). DN3- and proB-derived myeloid cells harbored V-DJ rearranged TCR genes and IgH genes, respectively, confirming that they had originated from T and B lineage progenitors (supplemental Figure 16B-C). We also observed lineage conversion from proB cells into myeloid cells via B-1 stage *in vitro* (supplemental Figure 16D-E), which was consistent with the increase in number of B-1 cells in BM chimera mice (Figure 5C; supplemental Figure 14F). We previously reported that *Ring1a/b* KO by *LckCre* converted T cells into B cells[53]. We again

analyzed *LckCre-Cdkn2a*$^{-/-}$*Ring1a*$^{-/-}$*Ring1b*$^{fl/fl}$ mice, and found that *Ring1a/b* KO DN3 cells expressed CD19 but some of them were B-1 phenotype lacking B220 expression (supplemental Figure 16F). DN3 cells of *LckCre* mice were also converted into myeloid cells via B lineage cells carrying rearranged *Igh* and *Tcrb* genes (supplemental Figure 16G-J). While *Ring1b* deletion converted non-phagocytic lineage cells into phagocytes, Ring1B overexpression did not convert phagocytes into non-phagocytic lineage cells (supplemental Figure 17A-E), indicating that polycomb complex plays roles in maintenance of non-phagocytic lineages but not in induction of non-phagocytic lineages.

We finally found that expression levels of Ring1A/B homologs were low in Capsaspora (Figure 6D), and *Ring1a/b* KO myeloid cells were more similar with Capsaspora than normal myeloid cells (Figure 6E). These data suggested that *Ring1a/b* KO reverted mouse cells toward a primordial status nearby Capsaspora, and that Ring1A/B has played roles in acquiring new lineages in evolution.

Discussion

Animals evolved from unicellular organisms[29,30,54-57], and Capsaspora, which is known to exhibit typical filopodial features is phylogenetically close to animals[15,20,58-61]. The present study enabled us to envisage that the phenotype of Capsaspora represents the origin of phagocytes in animals. We showed that Capsaspora has phagocytic potential and exhibit gene expression profiles similar to phagocytes of animals characterized by high CEBPα expression. We further showed that CEBPα homologs converted murine non-phagocyte progenitors into phagocytes.

Here we propose the following scenario in the evolutionary history of blood

419 cells: when a unicellular ancestor came to form a multicellular organism, a body cavity
420 structure surrounded by epithelium should have been formed. In such a situation it
421 would have been advantageous if the organism had an ancestral type of cell in the cavity
422 that was able to patrol it to eliminate pathogens and dead cells by phagocytosis. Thus,
423 the multicellular organism should have survived after succeeding in holding such cells
424 by inheriting the ancestral program for phagocytic characteristics driven by CEBPα,
425 bringing about the birth of the initial blood cells (Figure 7).

426 Thereafter, megakaryocyte, erythroid, T cell, and B cell lineages were
427 generated during the evolution of animals. An early study reported that the sea urchin
428 has blood cells with clotting function[62], so it is probable that the megakaryocyte lineage
429 had been segregated at an earlier stage than echinoderms in the branch of Deuterostomia.
430 An early branch of the megakaryocyte lineage in hematopoietic differentiation
431 pathway[63] should reflect its evolutionary early segregation. In chordates, at the level of
432 protochordates, blood cells are segregated into several lineages[5,64], and, in accordance
433 with this finding, we showed that CEBPα is specifically expressed in the phagocytic
434 blood cells. In the evolutionary history of vertebrates, before branching into jawless and
435 jawed fish, the erythroid and lymphoid lineages should have arisen, since both jawless
436 and jawed fish have these two cell types[65-67]. In vertebrate hematopoiesis, CEBPα is
437 specifically expressed in phagocytes, and it is now clear based on the present study that
438 repression of CEBPα to maintain non-phagocytic lineages is commonly achieved by
439 polycomb complex in vertebrates (Figure 7). The findings that Ring1*a/b* KO leads to
440 leukemogenesis in absence of Cdkn2a further suggested that Cdkn2a has been
441 employed for secure hematopoiesis, so that dysfunction of polycomb complex results in

apoptosis (Figure 5J; supplemental Figure 15D).

In vertebrate hematopoiesis, phagocytic blood lineages and CEBPα has been also diverged. It is known that quadruplication of genome took place in an ancestor of vertebrates after segregation from tunicates[68,69], and vertebrates have quadruple CEBPα genes: CEBPα, CEBPβ, CEBPδ, and CEBPε. Such quadruplication of CEBPα has enabled vertebrates to acquire various phagocytic blood cells; e.g. CEBPδ and CEBPε are important in granulocyte[46,70,71]. Homologs of other TFs essential to myeloid cells in vertebrates, such as PU.1 and IRF, were not found in Capsaspora (supplemental Figure 8B). It is probable that these genes have emerged after multicellular organisms had evolved from unicellular organisms, and have enabled vertebrates to acquire another phagocytic blood cells; e.g., dendritic cells.

We further argue whether findings in the present study shows some implications about multicellularization in ancestral unicellular organisms. Phagocytosis itself is common among some unicellular eukaryotes[72,73], but CEBP homologs has been found only in Filozoa[60]. Acquisition of CEBPα in ancestral Filozoan organisms, together with cis-regulatory system[61], should have enabled them to regulate a phagocytic program. Lower expression of CEBPα homolog and higher expression of Ring1A/B homologs in aggregative stage of Capsaspora than filopodial stage (Figure 2F, 6D) suggested that polycomb complex has played roles in repressing CEBPα and a phagocytic program in ancestral Filozoa. It is tempting to speculate that polycomb-mediated CEBPα repression has contributed to aggregation and multicellularization.

Of note was that hepatocytes, fibroblasts, and adipocyte, in which CEBPα is

also known to be expressed, showed similarity with Capsaspora. Since these cells are known to have phagocytic potential, it is likely that these cells also inherited Capsaspora program driven by CEBPα. Further study is required to unveil whether such programs has been seamlessly maintained in evolutionary history of these cells. Another unsolved issue is evolutionary history of Protostomia blood cells. It remains to be clarified whether they have seamlessly inherited the CEBPα-driven program, or have inherited an alternative one driven by different TFs.

Overall, the present study has provided insight into the origin of blood cells in the animal kingdom, where the primary phagocytes in the ancestor of animals arose by activating the CEBPα-driven phagocytic program inherited from a unicellular organism, and has clarified the molecular mechanism by which the phagocytic program is suppressed to maintain non-phagocytic lineage cells in vertebrate hematopoiesis, i.e., polycomb-mediated epigenetic suppression of CEBPα.

Acknowledgments

We thank Shimon Sakaguchi (Osaka University) for kindly providing *Rag2*$^{-/-}$ mice; Haruhiko Koseki (RIKEN) and Miguel Vidal (Centro de Investigaciones Biologicas) for kindly providing *Ert2Cre* mice and *Cdkn2a*$^{-/-}$*Ring1a*$^{-/-}$*Ring1b*$^{fl/fl}$ mice; Jun-ichi Miyazaki (Osaka University) for kindly providing *CAG*$^{flox\text{-}stop\text{-}GFP}$ mice; Ellen V. Rothenberg (Caltech) and Hiroyuki Hosokawa (Tokai University) for kindly providing the pMXs-IRES-hNGFR vector; and Peter Burrows (University of Alabama at Birmingham) for critical reading of the manuscript.

This work was supported by funds from Japan Society for the Promotion of Science KAKENHI, Grant-in-Aid for Scientific Research (B) (JP15H04743), and Grant-in-Aid for Scientific Research on Innovative Areas (JP 19H05747). LiMe Office of Director's Research Grants 2022 (No. 6) also supported this work.

Author Contribution

Y. Nagahata and H.K. conceived and designed the project. Y. Nagahata, K.M., T.I., Y. Nishimura, and S.K. designed and optimized experimental methodologies using mice, Y. Nagahata and Y.S. did so using tunicates, and Y. Nagahata and H.S. did so using Capsaspora. Y. Nagahata, H.S., and Y.S. performed experiments. Y. Nagahata, H.S., Y.S. analyzed the data. T.K., Y. Nannya, S.O., and A.T.-K gave advice in performing the experiments. Y. Nagahata., K.M., and H.K. wrote the paper.

Disclosure of Conflict of Interest

The authors declare no conflicts of interest.

References

1. Mukherjee S, Ray M, Ray S. Phagocytic efficiency and cytotoxic responses of Indian freshwater sponge (Eunapius carteri) cells isolated by density gradient centrifugation and flow cytometry: a morphofunctional analysis. *Zoology (Jena)*. 2015;118(1):8-18.

2. Kawamoto H, Ikawa T, Masuda K, Wada H, Katsura Y. A map for lineage restriction of progenitors during hematopoiesis: the essence of the myeloid-based model. *Immunol Rev*. 2010;238(1):23-36.

3. Cooper MD, Alder MN. The evolution of adaptive immune systems. *Cell*. 2006;124(4):815-822.

4. Boehm T. Evolution of vertebrate immunity. *Curr Biol*. 2012;22(17):R722-732.

5. Rosental B, Kowarsky M, Seita J, et al. Complex mammalian-like haematopoietic system found in a colonial chordate. *Nature*. 2018;564(7736):425-429.

6. Katsura Y, Kawamoto H. Stepwise lineage restriction of progenitors in lympho-myelopoiesis. *Int Rev Immunol*. 2001;20(1):1-20.

7. Kawamoto H, Ohmura K, Katsura Y. Direct evidence for the commitment of hematopoietic stem cells to T, B and myeloid lineages in murine fetal liver. *Int Immunol*. 1997;9(7):1011-1019.

8. Lu M, Kawamoto H, Katsube Y, Ikawa T, Katsura Y. The common myelolymphoid progenitor: a key intermediate stage in hemopoiesis generating T and B cells. *J Immunol*. 2002;169(7):3519-3525.

9. Masuda K, Kakugawa K, Nakayama T, Minato N, Katsura Y, Kawamoto H. T Cell Lineage Determination Precedes the Initiation of TCR Gene Rearrangement. *The Journal of Immunology*. 2007;179(6):3699-3706.

525 10. Wada H, Masuda K, Satoh R, et al. Adult T-cell progenitors retain myeloid
526 potential. *Nature*. 2008;452(7188):768-772.
527 11. Kawamoto H. A close developmental relationship between the lymphoid and
528 myeloid lineages. *Trends Immunol*. 2006;27(4):169-175.
529 12. Li J, Barreda DR, Zhang YA, et al. B lymphocytes from early vertebrates have
530 potent phagocytic and microbicidal abilities. *Nat Immunol*. 2006;7(10):1116-1124.
531 13. Nagasawa T, Nakayasu C, Rieger AM, Barreda DR, Somamoto T, Nakao M.
532 Phagocytosis by Thrombocytes is a Conserved Innate Immune Mechanism in Lower
533 Vertebrates. *Front Immunol*. 2014;5:445.
534 14. Stokes EE, Firkin BG. Studies of the peripheral blood of the Port Jackson shark
535 (Heterodontus portusjacksoni) with particular reference to the thrombocyte. *Br J*
536 *Haematol*. 1971;20(4):427-435.
537 15. Sebe-Pedros A, Irimia M, Del Campo J, et al. Regulated aggregative
538 multicellularity in a close unicellular relative of metazoa. *Elife*. 2013;2:e01287.
539 16. Consortium F, the RP, Clst, et al. A promoter-level mammalian expression atlas.
540 *Nature*. 2014;507(7493):462-470.
541 17. Choi J, Baldwin TM, Wong M, et al. Haemopedia RNA-seq: a database of gene
542 expression during haematopoiesis in mice and humans. *Nucleic Acids Res*.
543 2019;47(D1):D780-D785.
544 18. Imai KS, Hino K, Yagi K, Satoh N, Satou Y. Gene expression profiles of
545 transcription factors and signaling molecules in the ascidian embryo: towards a
546 comprehensive understanding of gene networks. *Development*.
547 2004;131(16):4047-4058.
548 19. Satou Y, Kawashima T, Shoguchi E, Nakayama A, Satoh N. An integrated

549 database of the ascidian, Ciona intestinalis: towards functional genomics. *Zoolog Sci*.
550 2005;22(8):837-843.
551 20. Suga H, Chen Z, de Mendoza A, et al. The Capsaspora genome reveals a
552 complex unicellular prehistory of animals. *Nat Commun*. 2013;4:2325.
553 21. Sogabe S, Hatleberg WL, Kocot KM, et al. Pluripotency and the origin of
554 animal multicellularity. *Nature*. 2019;570(7762):519-522.
555 22. de Mendoza A, Suga H, Permanyer J, Irimia M, Ruiz-Trillo I. Complex
556 transcriptional regulation and independent evolution of fungal-like traits in a relative of
557 animals. *Elife*. 2015;4:e08904.
558 23. Fairclough SR, Chen Z, Kramer E, et al. Premetazoan genome evolution and
559 the regulation of cell differentiation in the choanoflagellate Salpingoeca rosetta.
560 *Genome Biol*. 2013;14(2):R15.
561 24. Emms DM, Kelly S. OrthoFinder: phylogenetic orthology inference for
562 comparative genomics. *Genome Biol*. 2019;20(1):238.
563 25. Ohmura K, Kawamoto H, Fujimoto S, Ozaki S, Nakao K, Katsura Y.
564 Emergence of T, B, and myeloid lineage-committed as well as multipotent hemopoietic
565 progenitors in the aorta-gonad-mesonephros region of day 10 fetuses of the mouse. *J*
566 *Immunol*. 1999;163(9):4788-4795.
567 26. Masuda K, Kubagawa H, Ikawa T, et al. Prethymic T-cell development defined
568 by the expression of paired immunoglobulin-like receptors. *EMBO J*.
569 2005;24(23):4052-4060.
570 27. Turner EC. Possible poriferan body fossils in early Neoproterozoic microbial
571 reefs. *Nature*. 2021;596(7870):87-91.
572 28. Erwin DH, Laflamme M, Tweedt SM, Sperling EA, Pisani D, Peterson KJ. The

573 Cambrian conundrum: early divergence and later ecological success in the early history
574 of animals. *Science*. 2011;334(6059):1091-1097.
575 29. Shalchian-Tabrizi K, Minge MA, Espelund M, et al. Multigene phylogeny of
576 choanozoa and the origin of animals. *PLoS One*. 2008;3(5):e2098.
577 30. Torruella G, Derelle R, Paps J, et al. Phylogenetic relationships within the
578 Opisthokonta based on phylogenomic analyses of conserved single-copy protein
579 domains. *Mol Biol Evol*. 2012;29(2):531-544.
580 31. Torruella G, de Mendoza A, Grau-Bove X, et al. Phylogenomics Reveals
581 Convergent Evolution of Lifestyles in Close Relatives of Animals and Fungi. *Curr Biol*.
582 2015;25(18):2404-2410.
583 32. Hartenstein V. Blood cells and blood cell development in the animal kingdom.
584 *Annu Rev Cell Dev Biol*. 2006;22:677-712.
585 33. Soji T, Murata Y, Ohira A, Nishizono H, Tanaka M, Herbert DC. Evidence that
586 hepatocytes can phagocytize exogenous substances. *Anat Rec*. 1992;233(4):543-546.
587 34. Villena JA, Cousin B, Penicaud L, Casteilla L. Adipose tissues display
588 differential phagocytic and microbicidal activities depending on their localization. *Int J*
589 *Obes Relat Metab Disord*. 2001;25(9):1275-1280.
590 35. Romana-Souza B, Chen L, Leonardo TR, Chen Z, DiPietro LA. Dermal
591 fibroblast phagocytosis of apoptotic cells: A novel pathway for wound resolution.
592 *FASEB J*. 2021;35(4):e21443.
593 36. Molkentin JD, Kalvakolanu DV, Markham BE. Transcription factor GATA-4
594 regulates cardiac muscle-specific expression of the alpha-myosin heavy-chain gene. *Mol*
595 *Cell Biol*. 1994;14(7):4947-4957.
596 37. Milatovich A, Qiu RG, Grosschedl R, Francke U. Gene for a tissue-specific

transcriptional activator (EBF or Olf-1), expressed in early B lymphocytes, adipocytes, and olfactory neurons, is located on human chromosome 5, band q34, and proximal mouse chromosome 11. *Mamm Genome*. 1994;5(4):211-215.

38. Liu X, Rowan SC, Liang J, et al. Categorization of lung mesenchymal cells in development and fibrosis. *iScience*. 2021;24(6):102551.

39. Nerlov C, Graf T. PU.1 induces myeloid lineage commitment in multipotent hematopoietic progenitors. *Genes Dev*. 1998;12(15):2403-2412.

40. Tsujimura H, Tamura T, Gongora C, et al. ICSBP/IRF-8 retrovirus transduction rescues dendritic cell development in vitro. *Blood*. 2003;101(3):961-969.

41. Shayman JA, Tesmer JJG. Lysosomal phospholipase A2. *Biochim Biophys Acta Mol Cell Biol Lipids*. 2019;1864(6):932-940.

42. Mota AC, Dominguez M, Weigert A, Snodgrass RG, Namgaladze D, Brune B. Lysosome-Dependent LXR and PPARdelta Activation Upon Efferocytosis in Human Macrophages. *Front Immunol*. 2021;12:637778.

43. Xie H, Ye M, Feng R, Graf T. Stepwise reprogramming of B cells into macrophages. *Cell*. 2004;117(5):663-676.

44. Laiosa CV, Stadtfeld M, Xie H, de Andres-Aguayo L, Graf T. Reprogramming of committed T cell progenitors to macrophages and dendritic cells by C/EBP alpha and PU.1 transcription factors. *Immunity*. 2006;25(5):731-744.

45. Collombet S, van Oevelen C, Sardina Ortega JL, et al. Logical modeling of lymphoid and myeloid cell specification and transdifferentiation. *Proc Natl Acad Sci U S A*. 2017;114(23):5792-5799.

46. Cirovic B, Schonheit J, Kowenz-Leutz E, et al. C/EBP-Induced Transdifferentiation Reveals Granulocyte-Macrophage Precursor-like Plasticity of B

621 Cells. *Stem Cell Reports*. 2017;8(2):346-359.

622 47. Suh HC, Gooya J, Renn K, Friedman AD, Johnson PF, Keller JR. C/EBPalpha
623 determines hematopoietic cell fate in multipotential progenitor cells by inhibiting
624 erythroid differentiation and inducing myeloid differentiation. *Blood*.
625 2006;107(11):4308-4316.

626 48. Zhang DE, Zhang P, Wang ND, Hetherington CJ, Darlington GJ, Tenen DG.
627 Absence of granulocyte colony-stimulating factor signaling and neutrophil development
628 in CCAAT enhancer binding protein alpha-deficient mice. *Proc Natl Acad Sci U S A*.
629 1997;94(2):569-574.

630 49. Zhang P, Iwasaki-Arai J, Iwasaki H, et al. Enhancement of hematopoietic stem
631 cell repopulating capacity and self-renewal in the absence of the transcription factor
632 C/EBP alpha. *Immunity*. 2004;21(6):853-863.

633 50. Giladi A, Paul F, Herzog Y, et al. Single-cell characterization of haematopoietic
634 progenitors and their trajectories in homeostasis and perturbed haematopoiesis. *Nat Cell*
635 *Biol*. 2018;20(7):836-846.

636 51. Piunti A, Shilatifard A. Epigenetic balance of gene expression by Polycomb
637 and COMPASS families. *Science*. 2016;352(6290):aad9780.

638 52. Wang H, Wang L, Erdjument-Bromage H, et al. Role of histone H2A
639 ubiquitination in Polycomb silencing. *Nature*. 2004;431(7010):873-878.

640 53. Ikawa T, Masuda K, Endo TA, et al. Conversion of T cells to B cells by
641 inactivation of polycomb-mediated epigenetic suppression of the B-lineage program.
642 *Genes Dev*. 2016;30(22):2475-2485.

643 54. Sebe-Pedros A, Degnan BM, Ruiz-Trillo I. The origin of Metazoa: a unicellular
644 perspective. *Nat Rev Genet*. 2017;18(8):498-512.

645 55. Cavalier-Smith T, Chao EE. Phylogeny of choanozoa, apusozoa, and other
646 protozoa and early eukaryote megaevolution. *J Mol Evol*. 2003;56(5):540-563.
647 56. Steenkamp ET, Wright J, Baldauf SL. The protistan origins of animals and
648 fungi. *Mol Biol Evol*. 2006;23(1):93-106.
649 57. Ros-Rocher N, Perez-Posada A, Leger MM, Ruiz-Trillo I. The origin of
650 animals: an ancestral reconstruction of the unicellular-to-multicellular transition. *Open*
651 *Biol*. 2021;11(2):200359.
652 58. Stibbs HH, Owczarzak A, Bayne CJ, DeWan P. Schistosome sporocyst-killing
653 Amoebae isolated from Biomphalaria glabrata. *J Invertebr Pathol*. 1979;33(2):159-170.
654 59. Owczarzak A, Stibbs HH, Bayne CJ. The destruction of Schistosoma mansoni
655 mother sporocysts in vitro by amoebae isolated from Biomphalaria glabrata: an
656 ultrastructural study. *J Invertebr Pathol*. 1980;35(1):26-33.
657 60. Sebe-Pedros A, de Mendoza A, Lang BF, Degnan BM, Ruiz-Trillo I.
658 Unexpected repertoire of metazoan transcription factors in the unicellular holozoan
659 Capsaspora owczarzaki. *Mol Biol Evol*. 2011;28(3):1241-1254.
660 61. Sebe-Pedros A, Ballare C, Parra-Acero H, et al. The Dynamic Regulatory
661 Genome of Capsaspora and the Origin of Animal Multicellularity. *Cell*.
662 2016;165(5):1224-1237.
663 62. Kindred JE. Phagocytosis and clotting in the Pperivisceral fluid of Arbacia. *The*
664 *Biological Bulletin*. 1921;41(3):144-152.
665 63. Yamamoto R, Morita Y, Ooehara J, et al. Clonal analysis unveils self-renewing
666 lineage-restricted progenitors generated directly from hematopoietic stem cells. *Cell*.
667 2013;154(5):1112-1126.
668 64. Parrinello D, Parisi M, Parrinello N, Cammarata M. Ciona robusta hemocyte

669 populational dynamics and PO-dependent cytotoxic activity. *Dev Comp Immunol*.
670 2020;103:103519.
671 65. Hagerstrand H, Danieluk M, Bobrowska-Hagerstrand M, et al. The lamprey
672 (Lampetra fluviatilis) erythrocyte; morphology, ultrastructure, major plasma membrane
673 proteins and phospholipids, and cytoskeletal organization. *Mol Membr Biol*.
674 1999;16(2):195-204.
675 66. Pancer Z, Amemiya CT, Ehrhardt GR, Ceitlin J, Gartland GL, Cooper MD.
676 Somatic diversification of variable lymphocyte receptors in the agnathan sea lamprey.
677 *Nature*. 2004;430(6996):174-180.
678 67. Bajoghli B, Guo P, Aghaallaei N, et al. A thymus candidate in lampreys. *Nature*.
679 2011;470(7332):90-94.
680 68. Ohno S. Evolution by gene duplication. Berline: Springer; 1970.
681 69. Furlong RF, Holland PW. Were vertebrates octoploid? *Philos Trans R Soc Lond*
682 *B Biol Sci*. 2002;357(1420):531-544.
683 70. Scott LM, Civin CI, Rorth P, Friedman AD. A novel temporal expression
684 pattern of three C/EBP family members in differentiating myelomonocytic cells. *Blood*.
685 1992;80(7):1725-1735.
686 71. Yamanaka R, Barlow C, Lekstrom-Himes J, et al. Impaired granulopoiesis,
687 myelodysplasia, and early lethality in CCAAT/enhancer binding protein
688 epsilon-deficient mice. *Proc Natl Acad Sci U S A*. 1997;94(24):13187-13192.
689 72. Cavalier-Smith T. The phagotrophic origin of eukaryotes and phylogenetic
690 classification of Protozoa. *Int J Syst Evol Microbiol*. 2002;52(Pt 2):297-354.
691 73. Yutin N, Wolf MY, Wolf YI, Koonin EV. The origins of phagocytosis and
692 eukaryogenesis. *Biol Direct*. 2009;4:9.

693

694 **Figure Legends**

695 **Figure 1. Phagocytes of mouse, tunicate, and sponge are transcriptionally similar**
696 **with a unicellular organism.**

697 (A) Phylogenetic tree of mouse, tunicate, sponge, choanoflagellate, Capsaspora,
698 Ichthyosporea, and fungi.

699 (B-C) Heatmap with Pearson correlation of various mouse cell lineages and Capsaspora.
700 Gene expression profiles were compared among 3 stages of Capsaspora and 30 mouse
701 lineages (B) or 15 lineages (C) based on 3237 conserved homologs. Transcriptome data
702 examined by RNA-seq (B) or CAGE method (C) were analyzed. PC, peritoneal cavity.

703 (D) PC analyses of various lineages or stages of four species: Capsaspora, sponge,
704 tunicate, and mouse. Expression levels of 3237 conserved homologs were normalized
705 and compared.

706 (E) Venn diagrams with the number of highly expressed genes in Capsaspora filopodial
707 stage or mouse macrophages compared with mouse ESCs.

708 (F) Frequency of genes shared by mouse various cell lineages among 325 highly
709 expressed genes in Capsaspora filopodial stage. Statistical significance of differences
710 between macrophage and the other lineages were also shown.

711 (G) Frequency of phagocytosis related genes among 325 genes highly expressed in
712 Capsaspora filopodial stage and 2252 genes low expressed in Capsaspora filopodial
713 stage compared with mouse ESCs. Frequency of phagocytosis and lysosome related
714 genes expressed higher in mouse macrophages than mouse ESCs were shown.
715 Frequency of those highly expressed in macrophages than mouse ESCs and
716 non-phagocytic blood cells were shown in red and black.

717 (H) Cytology of mouse phagocyte (left) and Capsaspora (right) was examined by

718 Wright-Giemsa staining.

719 (I-J) Phagocytic activity of Capsaspora was evaluated by engulfment of pHrodo-green

720 beads (I), and frequency of phagocytic cells was evaluated by flow cytometry (J). Data

721 are representative of 2 independent experiments.

722 * $p<0.05$, ** $p<0.01$, **** $p<0.0001$

723

724 **Figure 2. Phagocytes and a unicellular organism share a CEBPα-driven phagocytic**

725 **program.**

726 (A, D) Venn diagrams with the number of highly expressed genes (A) and TFs (D) in

727 Capsaspora or mouse macrophages compared with mouse ESCs and non-phagocytic

728 blood cells.

729 (B) Top 8 KEGG pathways involved in the 11 genes highly expressed in Capsaspora

730 and mouse macrophages compared with mouse ESCs and non-phagocytic blood cells.

731 (C) PC analyses of various lineages or stages of four species: Capsaspora, sponge,

732 tunicate, and mouse. Expression levels of 62 conserved TFs were compared.

733 (E) Heatmap of scaled expression levels (z-score) of TFs in Capsaspora, mouse

734 macrophages, mouse ESCs, and mouse non-phagocytic blood cells. Four TFs expressed

735 higher in Capsaspora or mouse macrophages than in mouse ESCs and non-phagocytic

736 blood cells were selected. Expression levels were scaled among the 8 cell groups.

737 (F) Expression levels of CEBPα homologs and PLA2G15 homologs in Capsaspora, and

738 mouse various cell lineages. Data are mean ± SEM. Statistical significance of

739 differences between 3 stages of Capsaspora were shown.

740 * $p<0.05$, ** $p<0.01$

741

Figure 3. Tunicate and sponge phagocytes highly express CEBPα homologs.

(A) Scatter plots of sponge archaeocytes with $\log_2$ (TPM+1) values. The X axes indicate sponge CEBPα and CEBPγ. The Y axes indicate total expression levels of phagocytosis related genes and PLA2G15. (CEBPα homologs were excluded from phagocytosis related genes in these analyses.)

(B) Expression levels with $\log_2$ (TPM+1) values of CEBPα, CEBPγ, and phagocytosis related genes in tunicate. Transcriptome data of phagocytes were examined by RNA-seq, and data of the other lineages were based on expressed sequence tag (EST) counts obtained from the Ghost Database (http://ghost.zool.kyoto-u.ac.jp/cgi-bin/gb2/gbrowse/kh/).

(C) Blood cells of tunicate was aspirated by cardiac puncture. Collected blood cells were incubated with pHrodo beads and analyzed by flow cytometry.

(D) Blood cells of tunicate were analyzed by flow cytometry based on their size, autofluorescence, and fluorescence of engulfed beads.

(E) Normalized expression levels (*Gapdh* = 1) of CEBPα, CEBPγ and PLA2G15 in various lineage blood cells of tunicate were evaluated by RT-qPCR. Data are mean ± SEM.

* $p<0.05$, *** $p<0.001$, **** $p<0.0001$

Figure 4. Function of CEBPα to drive the phagocyte program has been conserved from a unicellular organism.

(A) Mouse CEBPα and its homologs from tunicate, sponge and Capsaspora were transduced into proB cells, which were analyzed by flow cytometry 4 days later.

765 (B, E, H-I) proB cells (B), MkPs (E), ErPs (H) and DN3 cells (I) were transduced with
766 mouse, tunicate, sponge, or Capsaspora CEBPα and then examined by flow cytometry
767 for the indicated lineage markers. Data are representative of 2–4 independent
768 experiments.
769 (C, F) The $CD11b^{+}$ cells generated by transduction with various CEBPα homologs into
770 proB cells (C) and MkPs (F) were sorted and their cytology was examined by
771 Wright-Giemsa staining (left). Their phagocytic activity was evaluated by engulfment of
772 pHrodo-green beads (right).
773 (D, G) Phagocytic activities of the generated $CD11b^{+}$ cells from proB cells (D) and
774 MkPs (G) was evaluated by flow cytometry.
775 (J) Wright-Giemsa stain of neutrophil-like cells with ring-shaped or multi-lobulated
776 nuclei generated by transduction with mouse CEBPα into proB cells.
777 (K) Frequency of cell types evaluated by cytology with Wright-Giemsa staining. One
778 hundred cells transduced with mouse, tunicate or sponge CEBPα were examined.
779 (L) Relative expression of neutrophil-associated genes in proB cells 2 days after
780 CEBPα transduction. Relative expression levels (day0 =1) with $2^{-\Delta\Delta CT}$ values
781 normalized with β-actin were shown. Data are mean ± SEM of 3 replicates. ** $p<0.01$,
782 *** $p<0.001$
783
784 **Figure 5. Polycomb mediated suppression of CEBPα is required for maintenance**
785 **of various hematopoietic lineages in mouse.**
786 (A, I) Experimental procedure for conditional inactivation of polycomb function. BM
787 cells of *Ert2Cre-CAG*$^{flox\text{-}stop\text{-}GFP}$*-Cdkn2a*$^{-/-}$*Ring1a*$^{-/-}$*Ring1b*$^{fl/fl}$ mice or

Ert2Cre-CAG$^{flox\text{-}stop\text{-}GFP}$*-Cdkn2a*$^{-/-}$*Ring1a*$^{-/-}$*Ring1b*$^{fl/+}$ mice were transplanted without (a) or with (i) competitor cells by intravenous injection into sublethally irradiated *Rag2*$^{-/-}$ mice. Six weeks later, the transplanted mice were administrated tamoxifen intraperitoneally to delete *Ring1b* in blood cells. Two (A) or eight (I) weeks after *Ring1b* deletion, mice were sacrificed and analyzed.

(B-D) Flow cytometric profiles of GFP$^+$ thymocytes (B) and GFP$^+$ BM cells (C-D). Upper and lower panels show data of control (Δ/+; *Cdkn2a*$^{-/-}$*Ring1a*$^{-/-}$*Ring1b*$^{\Delta/+}$, $n = 5$ in B and D, and n = 3 in C) and *Ring1a/b* KO (Δ/Δ; *Cdkn2a*$^{-/-}$*Ring1a*$^{-/-}$*Ring1b*$^{\Delta/\Delta}$, $n = 6$ in B, $n = 3$ in C, and n = 5 in D) mice, respectively.

(E-G) Number of GFP$^+$ DN3 cells (E), proB cells (F), and ErPs and MkPs (G) of control (black) and *Ring1a/b* KO (red) mice.

(H) Survival curve with Kaplan-Meier plots after BM transplantation to sublethally irradiated *Rag2*$^{-/-}$ mice. Black and red lines show survival curve of control (*Cdkn2a*$^{-/-}$*Ring1a*$^{-/-}$*Ring1b*$^{\Delta/+}$, n = 4) and *Ring1a/b* KO (*Cdkn2a*$^{-/-}$*Ring1a*$^{-/-}$*Ring1b*$^{\Delta/\Delta}$, n = 3) mice, respectively. Statistical significance of differences between the survival rates were calculated with the Log-rank test.

(J) Flow cytometric profiles of whole BM cells of control (n = 4), *Ring1a/b* KO in *Cdkn2a*$^{-/-}$ background (n = 4), and *Ring1a/b* KO in *Cdkn2a*$^{+/-}$ background (n = 3) mice with competitor cells.

(K) Percentage of myeloid cells, RBCs, T cells, and B cells among GFP$^+$ BM cells of control (black) and *Ring1a/b* KO (red) mice with competitor cells.

(L) Wright-Giemsa stain of BM smears obtained from control and *Ring1a/b* KO mice with competitor cells.

Data are mean ± SEM.

* p<0.05, ** p<0.01, *** p<0.001, **** p<0.0001

Figure 6. Various lineage progenitors were reverted into the primordial lineage of phagocytes by *Ring1a/b* KO.

(A) DN3 cells, proB cells, ErPs, and MkPs isolated from *Ert2Cre-Cdkn2a*$^{-/-}$*Ring1a*$^{-/-}$*Ring1b*$^{fl/fl}$ mice were co-cultured with TSt4 or TSt4-DLL1 cells for 4 -12 days with or without 4-OHT in the presence of 10 ng/ml of SCF, Flt3-L, IL-1α, IL-3, IL-7, TNFα, and GM-CSF. For ErPs and MkPs, 2 U/ml of EPO and 50 ng/ml of TPO were added, respectively.

(B) Flow cytometric profiles of the cultured cells. Data are representative of 3 independent experiments.

(C) Cytology of the generated CD11b^{+} cells was examined by Wright-Giemsa staining (left), and their phagocytic activity was evaluated by pHrodo-green beads with CD11b-BV421 staining (right).

(D) Expression levels of Ring1A/B homologs in Capsaspora and mouse various cell lineages.

(E) Heatmap with Pearson correlation of mouse normal and *Ring1a/b* KO myeloid cells and Capsaspora.

Figure 7. Schematic illustration for the evolution of blood cells.

A component of the unicellular organism phenotype has been seamlessly inherited as phagocytes in multicellular animals. Vertebrates acquired various lineage blood cells by suppressing CEBPα using polycomb complexes. When polycomb function was

835 impaired, hematopoiesis was reverted into a primitive one with phagocytes alone.

836

Figure 1

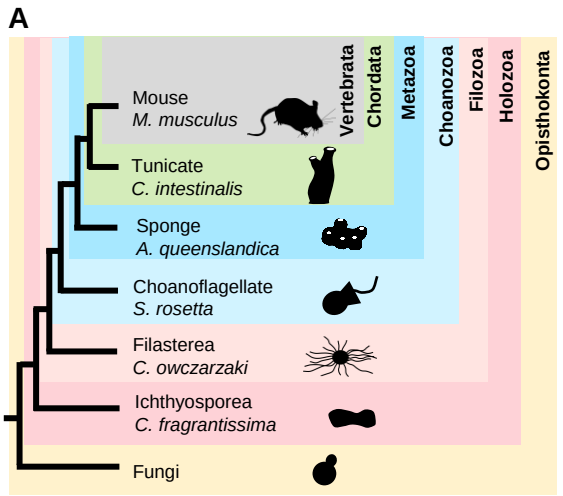

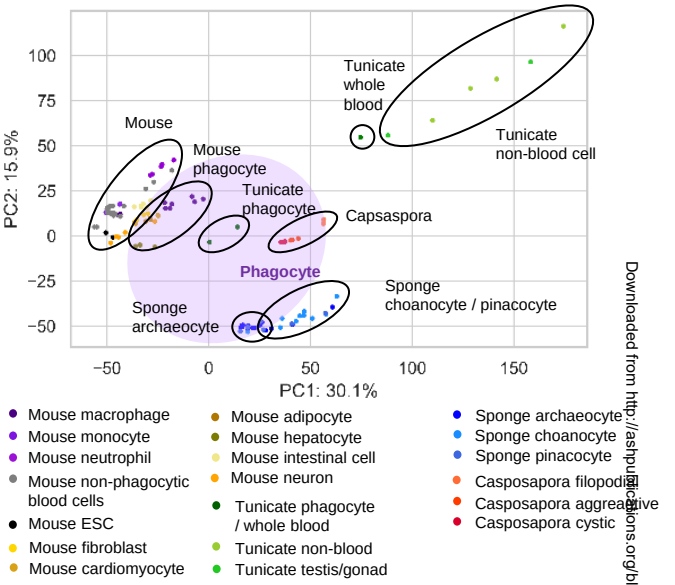

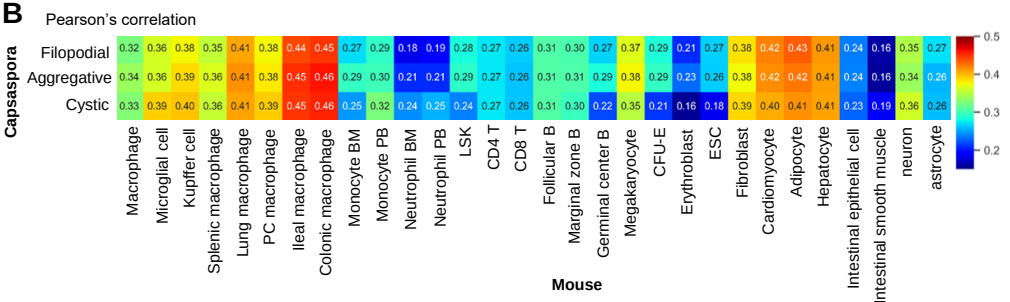

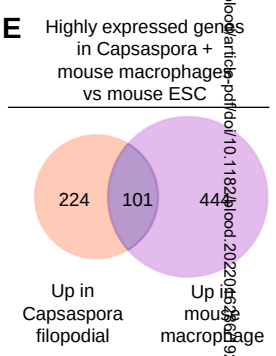

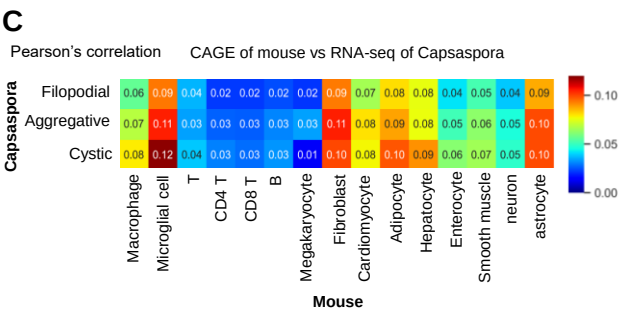

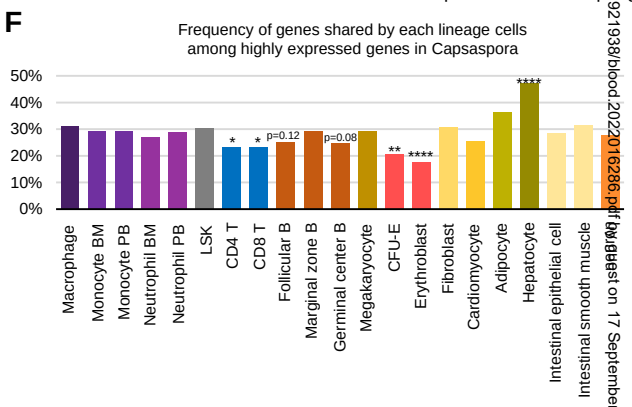

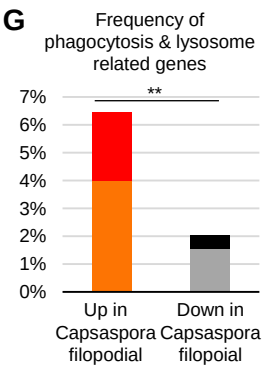

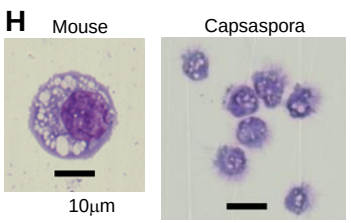

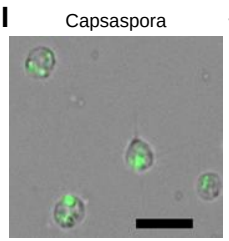

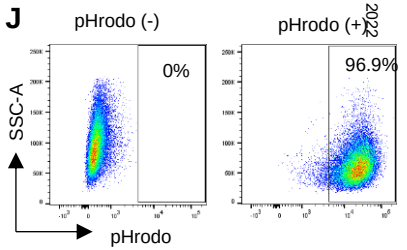

Figure 2

A

Highly expressed genes in Capsaspora + mouse macrophages vs mouse ESC/LSK/T/B/Mk/Er

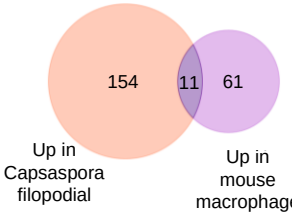

B

Top 8 KEGG pathways highly expressed in Capsaspora and mouse macrophage compared with mouse ESC/LSK/T/B/Mk/Er

mmu04142 Lysosome (3)
mmu05202 Transcriptional misregulation in cancer (3)
mmu04210 Apoptosis (2)
mmu04140 Autophagy - animal (2)
mmu00564 Glycerophospholipid metabolism (2)
mmu01100 Metabolic pathways (2)
mmu04612 Antigen processing and presentation (2)
mmu05221 Acute myeloid leukemia (2)

D

Highly expressed TFs in Capsaspora + mouse macrophages vs mouse ESC/LSK/T/B/Mk/Er

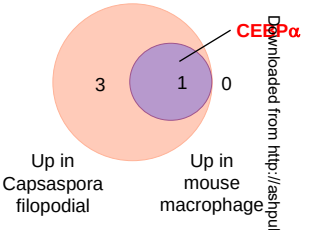

C

PC analysis with 62 conserved TFs among 4 species

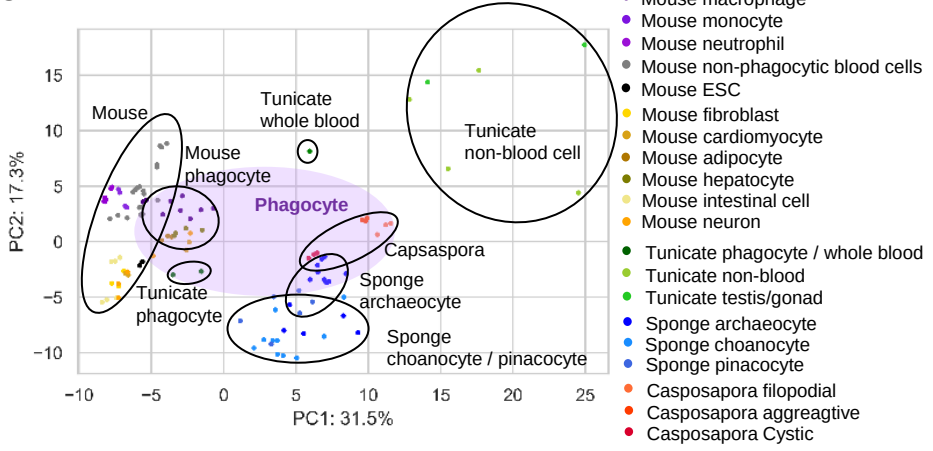

E

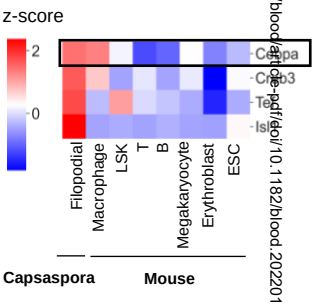

F

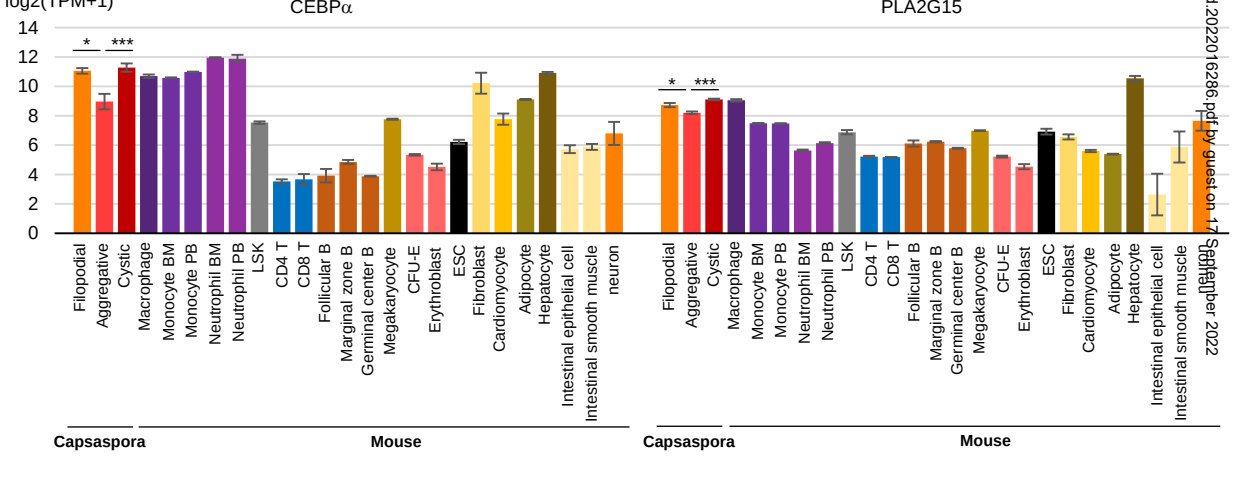

Figure 3

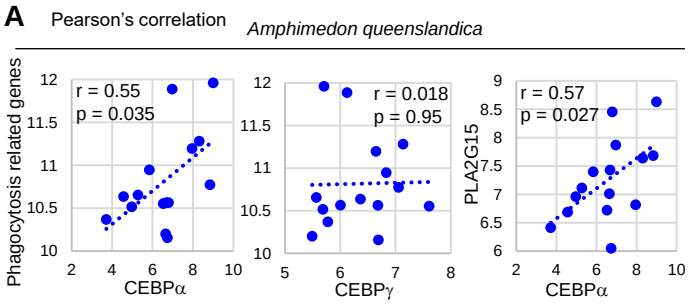

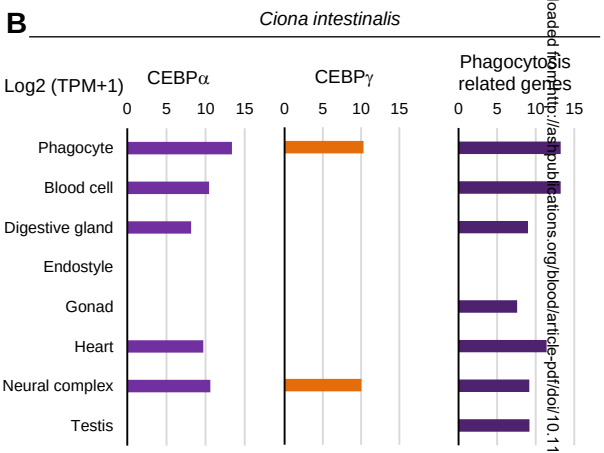

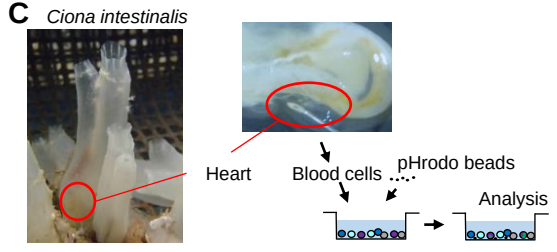

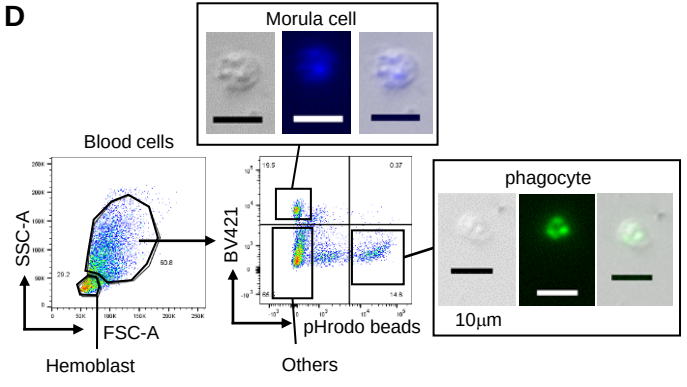

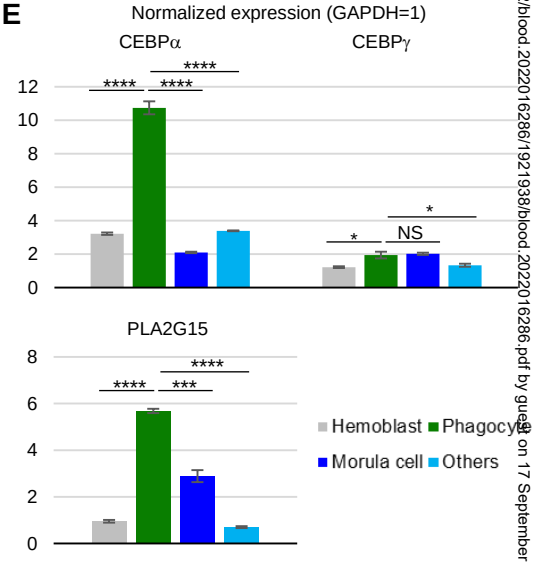

Figure 4

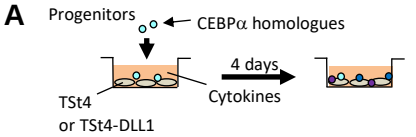

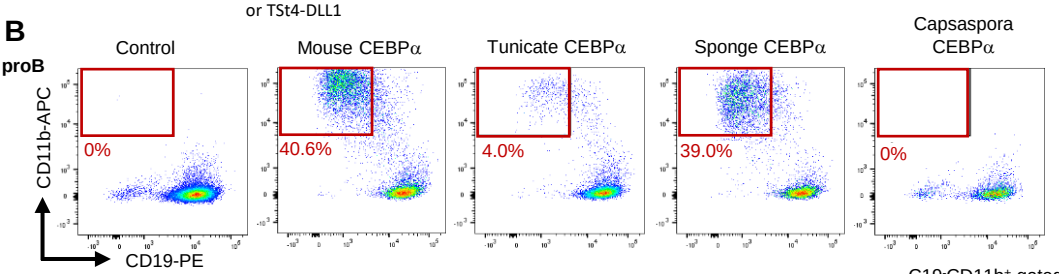

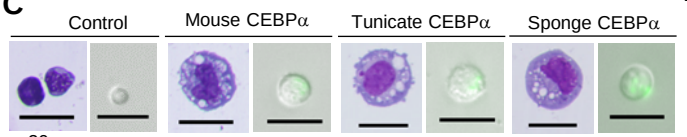

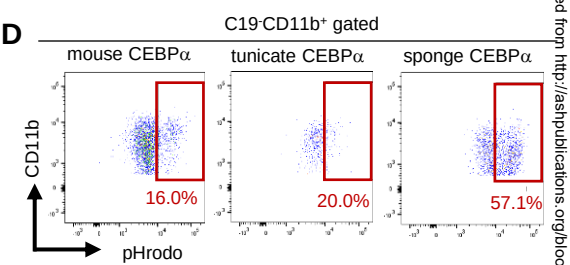

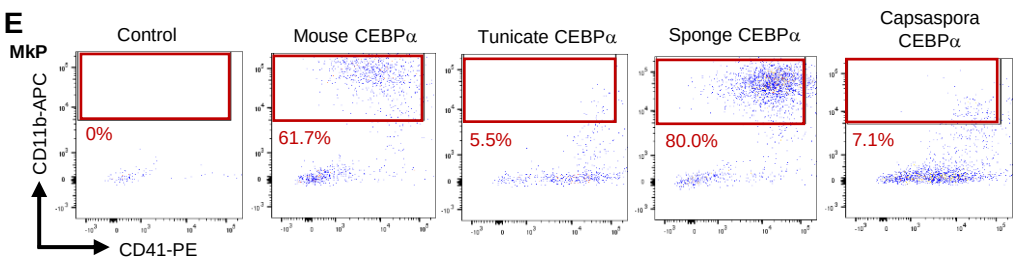

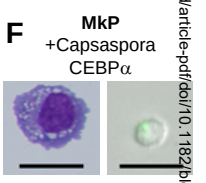

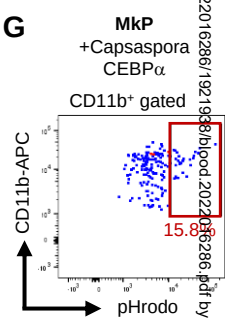

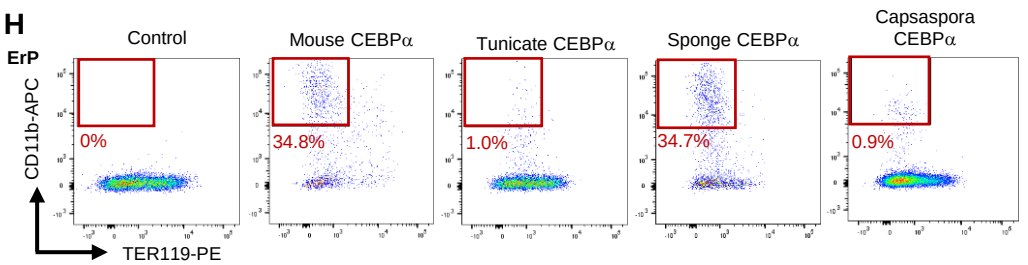

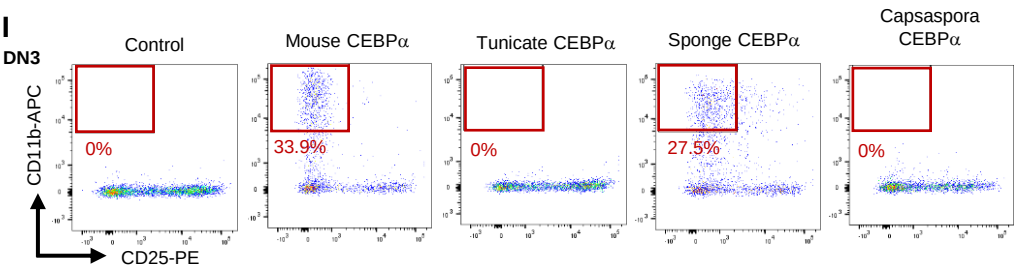

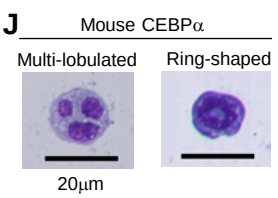

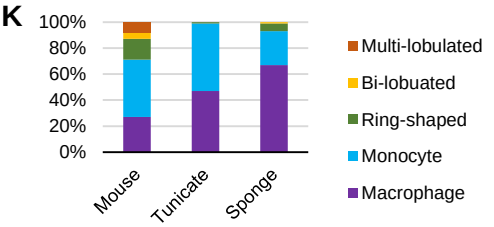

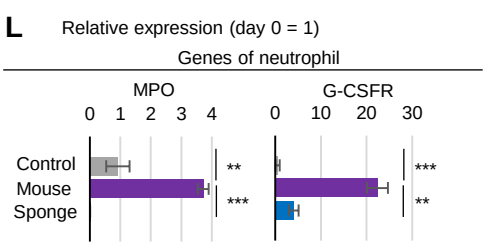

Figure 5

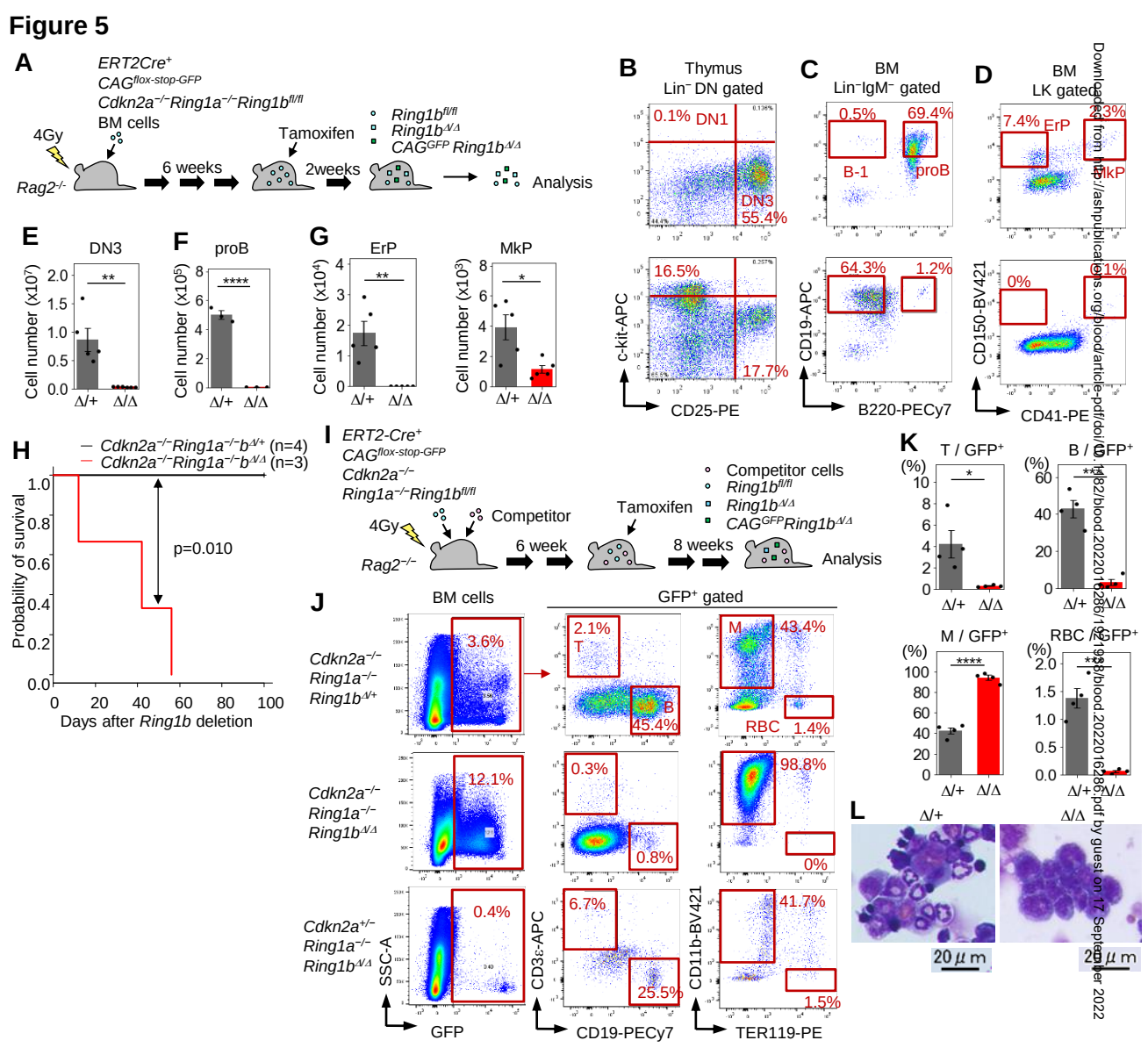

Figure 6

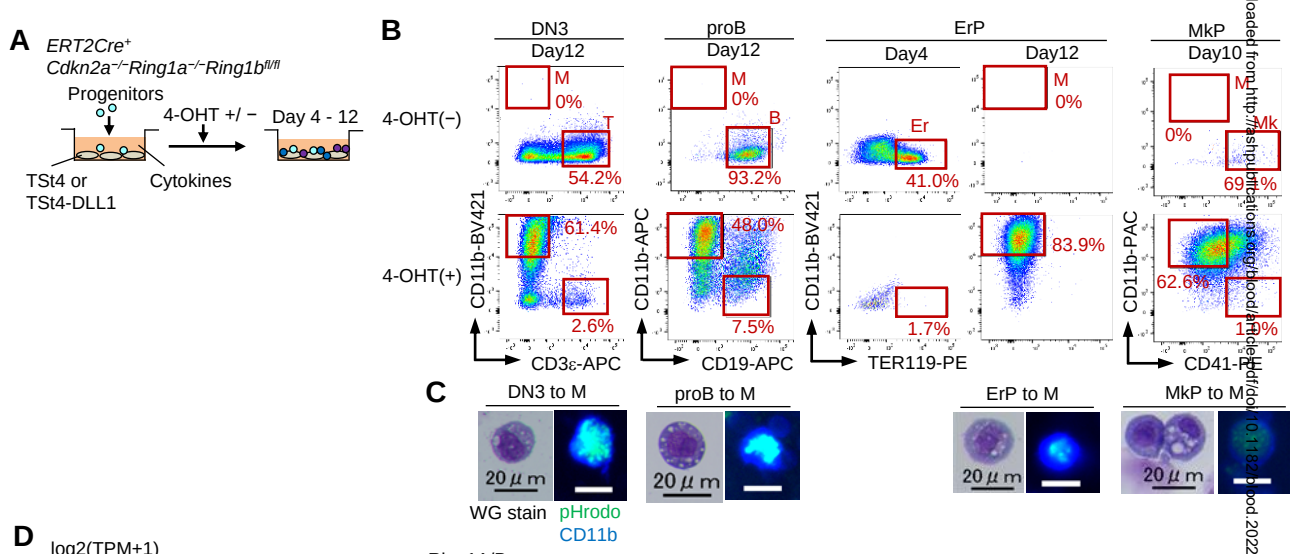

Figure 7